



# The Modified Kies Flexible Generalized Family: Properties, Simulations, and Applications

Alexandro A. Ferreira   
Federal University of Pernambuco  
Recife, Brazil

Gauss M. Cordeiro   
Federal University of Pernambuco  
Recife, Brazil

---

## Abstract

The modified Kies flexible generalized family is developed. It can incorporate bimodal and bathtub shapes, and its properties are derived from those of the exponentiated-G class. Within this family, a special case is discussed in terms of its properties and a regression model. The parameters are estimated using the maximum likelihood method, and some simulations are carried out to check their consistency. The usefulness of the proposals is proven by means of three real data sets.

*Keywords:* acceptance-rejection method, COVID-19, Kies distribution, regression model.

---

## 1. Introduction

The development of statistical distributions is a crucial area of research that aims to provide more suitable models for analyzing real-world data. Several flexible families have been proposed in recent years to overcome the limitations of existing models. Notable contributions in this field include the works of Marshall and Olkin (1997), Gupta, Gupta, and Gupta (1998), Eugene, Lee, and Famoye (2002), Zografos and Balakrishnan (2009), Cordeiro and de Castro (2011), Alexander, Cordeiro, Ortega, and Sarabia (2012), Cordeiro, Ortega, and Cunha (2013), Alzaatreh, Lee, and Famoye (2013), Bourguignon, Silva, and Cordeiro (2014), Alizadeh, Emadi, Doostparast, Cordeiro, Ortega, and Pescim (2015), Chipepa, Oluyede, and Makubate (2019), Baharith and Alamoudi (2021), and Tlhaloganyang, Sengweni, and Oluyede (2022), among many others.

Tahir, Hussain, and Cordeiro (2022) defined the cumulative distribution function (cdf) of the *flexible generalized family* (FGF) from the baseline cdf  $G(x) = G(x; \boldsymbol{\xi})$ , which requires no additional parameters (for  $x \in \mathbb{R}$ )

$$H(x) = H(x; \boldsymbol{\xi}) = 1 - \bar{G}(x)^{G(x)},$$

where  $\bar{G}(x) = 1 - G(x)$  and  $\boldsymbol{\xi}$  represents the vector of parameters of  $G(\cdot)$ .

The cdf of the *modified Kies flexible generalized* (MKF-G) family is defined from the Transformed-Transformer (T-X) class (Alzaatreh *et al.* 2013) and the two-parameter modified Kies cdf

(Kumar and Dharmaja 2017) with scale  $\lambda > 0$  and shape  $\beta > 0$  as (for  $x \in \mathbb{R}$ )

$$F(x) = 1 - \exp \left\{ -\lambda \left[ \bar{G}(x)^{-G(x)} - 1 \right]^\beta \right\}, \quad (1)$$

where its probability density function (pdf) reduces to

$$\begin{aligned} f(x) &= \lambda \beta g(x) \bar{G}(x)^{-\beta G(x)} \left[ 1 - \bar{G}(x)^{G(x)} \right]^{\beta-1} \left[ \frac{G(x)}{\bar{G}(x)} - \log \bar{G}(x) \right] \\ &\times \exp \left\{ -\lambda \left[ \bar{G}(x)^{-G(x)} - 1 \right]^\beta \right\}, \end{aligned} \quad (2)$$

where  $g(x) = dG(x)/dx$ . The hazard rate function (hrf) associated with (2) follows easily by  $h(x) = f(x)/[1 - F(x)]$ .

Henceforth, let  $X \sim \text{MKF-G}(\lambda, \beta, \xi)$  be a random variable with pdf (2). The main motivation for introducing the MKF-G family is its greater flexibility compared to the Kumaraswamy-G and beta-G classes. Specifically, the MKF-G family can accommodate bimodal and bathtub shapes in its baseline distributions as illustrated in Figures 1, 2, and 3. This feature allows this family to model real-world data that exhibits these complex shapes more effectively as demonstrated in Section 6.

The article presents the following topics. Section 2 discusses three special models of the new family. Section 3 describes its main properties. Section 4 provides some properties and a regression model for a special case of the new family. Simulations are reported in Section 5. Section 6 presents three applications to real data, and some conclusions are addressed in Section 7.

## 2. Some special models

The densities of three models belonging to the new family are presented. All plots are produced in R (R Core Team 2023).

### 2.1. The modified Kies flexible Weibull (MKFW)

Considering the Weibull baseline with shape  $\alpha > 0$  and scale  $\tau > 0$ , the MKFW density has the form

$$\begin{aligned} f(x) &= \lambda \beta \alpha \tau^{-\alpha} x^{\alpha-1} e^{-(x/\tau)^\alpha} \exp \left\{ \beta \left[ 1 - e^{-(x/\tau)^\alpha} \right] (x/\tau)^\alpha \right\} \\ &\times \left[ 1 - \exp \left\{ - \left[ 1 - e^{-(x/\tau)^\alpha} \right] (x/\tau)^\alpha \right\} \right]^{\beta-1} \left\{ \left[ e^{(x/\tau)^\alpha} - 1 \right] + (x/\tau)^\alpha \right\} \\ &\times \exp \left\{ -\lambda \left[ e^{(1-e^{-(x/\tau)^\alpha})(x/\tau)^\alpha} - 1 \right]^\beta \right\}. \end{aligned} \quad (3)$$

### 2.2. The modified Kies flexible Kumaraswamy (MKFKw)

For the Kumaraswamy (Kw) baseline with positive shape parameters  $a$  and  $b$ , the MKFKw density can be expressed from (2) as

$$\begin{aligned} f(x) &= \lambda \beta a b x^{a-1} (1-x)^{b-1} \left[ (1-x)^b \right]^{-\beta [1-(1-x^a)^b]} \left\{ 1 - \left[ (1-x^a)^b \right]^{[1-(1-x^a)^b]} \right\}^{\beta-1} \\ &\times \left\{ \left[ (1-x^a)^{-b} - 1 \right] - b \log(1-x^a) \right\} \exp \left\{ -\lambda \left[ \left[ (1-x^a)^b \right]^{-[1-(1-x^a)^b]} - 1 \right]^\beta \right\}. \end{aligned}$$

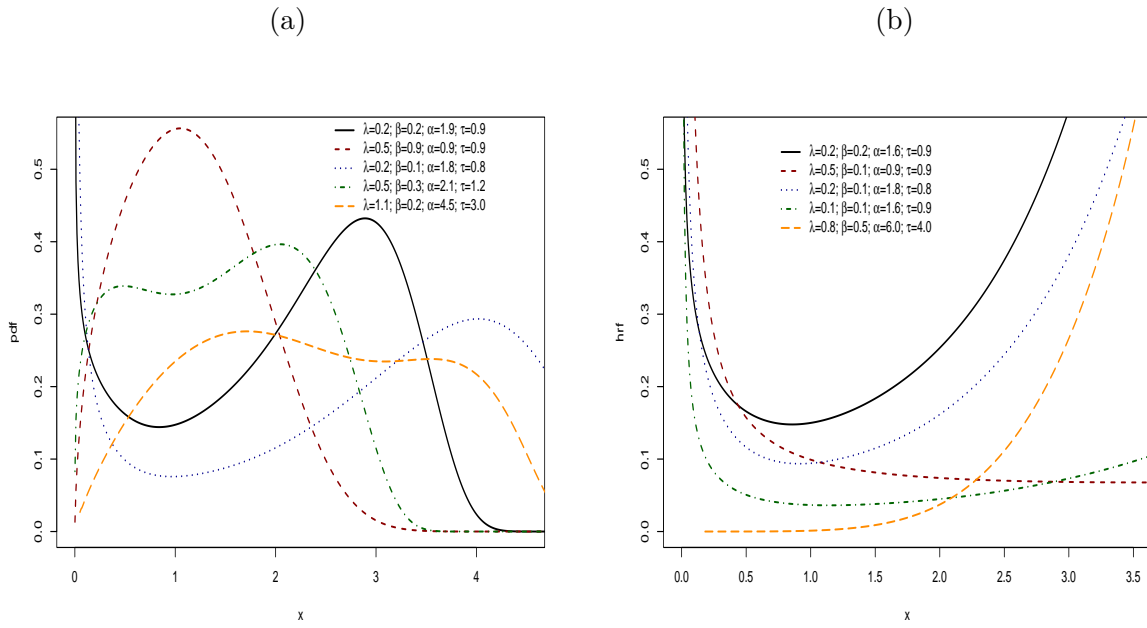


Figure 1: Density and hrf of  $MKFW(\lambda, \beta, \alpha, \tau)$

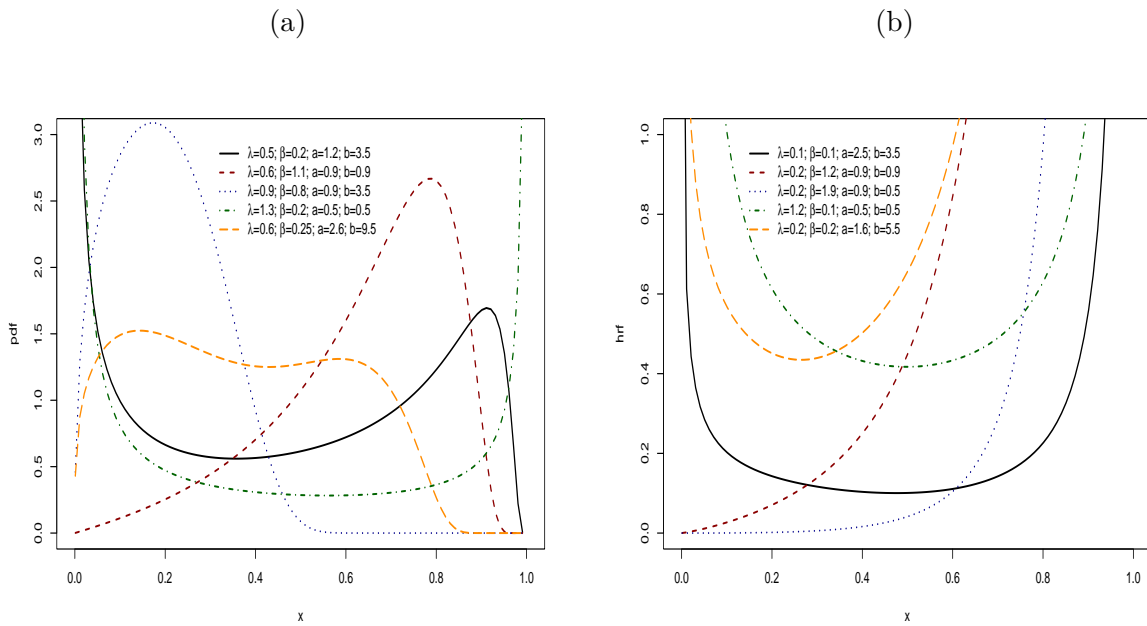


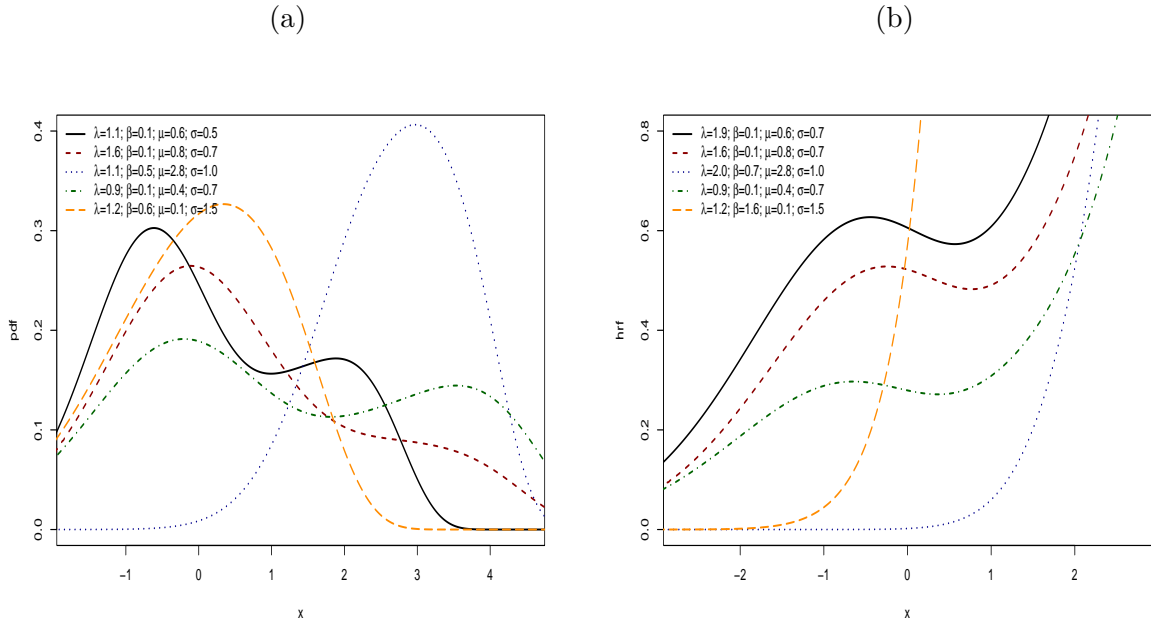
Figure 2: Density and hrf of  $MKFKw(\lambda, \beta, a, b)$

### 2.3. The modified Kies flexible normal (MKFN)

The MKFN density follows from the normal baseline  $N(\mu, \sigma^2)$  (for  $\mu \in \mathbb{R}$ , and  $\sigma > 0$ ) as

$$f(x) = \lambda \beta \phi(z) [1 - \Phi(z)]^{-\beta \Phi(z)} \left\{ 1 - [1 - \Phi(z)]^{\Phi(z)} \right\}^{\beta-1} \left\{ \frac{\Phi(z)}{1 - \Phi(z)} - \log [1 - \Phi(z)] \right\} \\ \times \exp \left\{ -\lambda \left( [1 - \Phi(z)]^{-\Phi(z)} - 1 \right)^\beta \right\}, \quad x \in \mathbb{R},$$

where  $z = (x - \mu) / \sigma$ , and  $\phi(\cdot)$  and  $\Phi(\cdot)$  are the pdf and cdf of the standard normal, respectively. Figures 1, 2, and 3 report density shapes and hrfs for three selected models. These pdfs can accommodate right-skewed, left-skewed, decreasing-increasing-decreasing, and particularly bimodal data, while their hrfs exhibit decreasing, increasing, and bathtub shapes.

Figure 3: Density and hrf of MKFN( $\lambda, \beta, \mu, \sigma^2$ )

### 3. Properties

#### 3.1. Linear representation

The exponentiated-G (exp-G) class has been widely researched in the past three decades. Several distributions belonging to this class have been proposed as those reported in Table 1 by [Tahir and Nadarajah \(2015\)](#). Its density for an arbitrary cdf  $G(x)$  with power  $\delta > 0$  is  $\pi_\delta = \delta g(x) G(x)^{\delta-1}$ .

Notable examples include the exp-exponential ([Gupta and Kundu 2001](#)), exp-Weibull ([Mudholkar and Srivastava 1993](#)), exp-Fréchet ([Nadarajah and Kotz 2003](#)), and exp-gamma ([Nadarajah and Gupta 2007](#)) distributions.

Initially, the generalized binomial expansion (for  $|v| < 1$ , and  $q \in \mathbb{R}$ ) holds

$$(1 - v)^q = \sum_{j=0}^{\infty} (-1)^j \binom{q}{j} v^j, \quad (4)$$

where  $\binom{q}{0} = 1$  and  $\binom{q}{j} = \frac{1}{j!} \prod_{n=1}^j (q - n + 1)$ , for  $j \geq 1$ .

Equation (1) can be rewritten as

$$F(x) = 1 - \exp \left\{ -\lambda \left( \frac{[1 - \bar{G}(x)^{G(x)}]^\beta}{\bar{G}(x)^{\beta G(x)}} \right) \right\}. \quad (5)$$

Next, applying (4) in Equation (5), since  $\bar{G}(x)^{G(x)} \in (0, 1)$ ,

$$F(x) = 1 - \exp \left\{ -\lambda \sum_{i=0}^{\infty} (-1)^i \binom{\beta}{i} [1 - G(x)]^{(i-\beta)G(x)} \right\}. \quad (6)$$

The Taylor series expansion of  $(1 - v)^{pv}$  at  $v = 0$  (for any real  $p$ ) is

$$(1 - v)^{pv} = \sum_{n=0}^{\infty} c_n v^n, \quad |v| < 1, \quad (7)$$

where  $c_0 = 1, c_1 = 0, c_2 = -p, c_3 = -p/2, c_4 = (3p^2 - 2p)/6, c_5 = (2p^2 - p)/4$ , etc. By inserting (7) in Equation (6),

$$F(x) = 1 - \exp \left\{ -\lambda \sum_{j=0}^{\infty} b_j G(x)^j \right\},$$

where

$$b_j = b_j(\beta) = \sum_{i=0}^{\infty} (-1)^i \binom{\beta}{i} c_j,$$

and the coefficients  $c_j$ 's follow from (7) by taking  $p = (i - \beta)$ . Thus, Theorem 25 of Munir (2013) gives

$$F(x) = 1 - \sum_{j=0}^{\infty} a_j G(x)^j, \quad (8)$$

where  $a_0 = \exp(-\lambda b_0)$  and  $a_j = (-\lambda/j) \sum_{k=1}^j k b_k a_{j-k}$  for  $j \geq 1$ . By differentiating (8), it follows the MKF-G density

$$f(x) = \sum_{j=0}^{\infty} \varphi_{j+1} \pi_{j+1}(x), \quad (9)$$

where  $\varphi_{j+1} = -a_{j+1}$ , and  $\pi_{j+1}(x)$  is the exp-G density with power  $j+1$ . Equation (9) reveals that the MKF-G density is an infinite linear combination of exp-G densities, which determines some of its properties.

### 3.2. Moments

The  $r$ th moment of  $X$ , say  $\mathbb{E}(X^r) = \int_{-\infty}^{\infty} x^r f(x) dx$ , can be written from (9) as

$$\mu'_r = \mathbb{E}(X^r) = \sum_{j=0}^{\infty} \varphi_{j+1} \mathbb{E}(Y_{j+1}^r) = \sum_{j=0}^{\infty} \varphi_{j+1} \int_0^1 Q_G(u)^r u^j du, \quad (10)$$

where  $Y_{j+1}$  is the density of the random variable exp-G( $j+1$ ).

The  $r$ th incomplete moment of  $X$ , say  $m_r(z) = \int_{-\infty}^z x^r f(x) dx$ , comes from (9) as

$$m_r(z) = \sum_{j=0}^{\infty} \varphi_{j+1} \int_{-\infty}^z x^r \pi_{j+1}(x) dx = \sum_{j=0}^{\infty} (j+1) \varphi_{j+1} \int_0^{G(z)} Q_G(u)^r u^j du. \quad (11)$$

The Bonferroni and Lorenz curves for a given probability  $\nu$  are  $B(\nu) = m_1(q)/\nu\mu'_1$  and  $L(\nu) = m_1(q)/\mu'_1$ , respectively, where  $q$  satisfies  $F(q) = \nu$  with  $F(\cdot)$  coming from (1).

### 3.3. Estimation

For a set of independent and identically distributed (iid) observations  $x_1, \dots, x_n$  from the pdf (2), the log-likelihood function for  $\boldsymbol{\theta} = (\lambda, \beta, \boldsymbol{\xi})^T$  has the form

$$\begin{aligned} \ell(\boldsymbol{\theta}) = & n [\log(\lambda) + \log(\beta)] + \sum_{i=1}^n \log g(x_i) - \beta \sum_{i=1}^n G(x_i) \log [1 - G(x_i)] \\ & + (\beta - 1) \sum_{i=1}^n \log \left\{ 1 - [1 - G(x_i)]^{G(x_i)} \right\} + \sum_{i=1}^n \log \left( \frac{G(x_i)}{1 - G(x_i)} - \log [1 - G(x_i)] \right) \\ & - \lambda \sum_{i=1}^n \left\{ [1 - G(x_i)]^{-G(x_i)} - 1 \right\}^\beta. \end{aligned} \quad (12)$$

The maximum likelihood estimate (MLE) of  $\theta$  can be found by maximizing (12) numerically using statistical software such as R, 0x or SAS.

#### 4. Main MKFW properties

The  $r$ th moment of  $X$  with pdf (3) can be determined by employing (10) and the findings of Nadarajah and Gupta (2005) (for  $r > -\alpha$ )

$$\mu'_r = \sum_{j=0}^{\infty} \sum_{\ell=0}^j \frac{(-1)^\ell (j+1) \tau^r}{(\ell+1)^{\frac{r}{\alpha}+1}} \binom{j}{\ell} \varphi_{j+1} \Gamma\left(\frac{r}{\alpha} + 1\right),$$

where  $\Gamma(\cdot)$  is the complete gamma function. Figure 4 displays the skewness and kurtosis plots of  $X$  for some parameter values. Both measures increase when  $\beta$  increases.

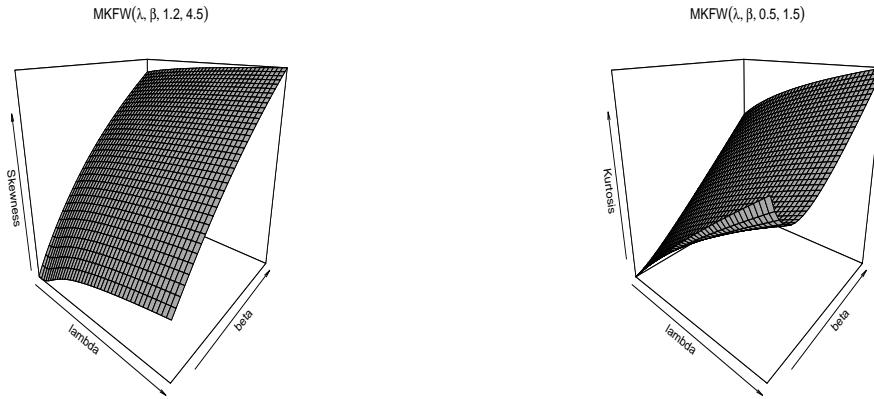


Figure 4: Skewness and kurtosis of  $\text{MKFW}(\lambda, \beta, \alpha, \tau)$

The  $r$ th incomplete moment of the MKFW distribution can be obtained from Equation (11) as (for  $r > -\alpha$ )

$$m_r(z) = \sum_{j=0}^{\infty} \sum_{\ell=0}^j \frac{(-1)^\ell (j+1) \tau^r}{(1+\ell)^{\frac{r}{\alpha}+1}} \binom{j}{\ell} \varphi_{j+1} \gamma\left(\frac{r}{\alpha} + 1, (\ell+1) \left[\frac{z}{\tau}\right]^\alpha\right),$$

where  $\gamma(\cdot, \cdot)$  is the lower incomplete gamma function. Figure 5 illustrates the Bonferroni and Lorenz curves for  $X$  given a probability  $\nu$  for some values of  $\lambda$  and  $\beta$ , with  $\tau = 0.2$  and  $\alpha = 0.3$ .

For iid observations  $x_1, \dots, x_n$  from the MKFW distribution, the log-likelihood function for  $\theta = (\lambda, \beta, \tau, \alpha)^\top$  reduces to

$$\begin{aligned} \ell(\theta) = & n [\log(\lambda) + \log(\beta) + \log(\alpha) - \alpha \log(\tau)] + (\alpha - 1) \sum_{i=1}^n \log(x_i) - \sum_{i=1}^n (x_i/\tau)^\alpha \\ & + \sum_{i=1}^n \left\{ \beta \left[ 1 - e^{-(x_i/\tau)^\alpha} \right] (x_i/\tau)^\alpha \right\} + \sum_{i=1}^n \log \left\{ \left[ e^{(x_i/\tau)^\alpha} - 1 \right] + (x_i/\tau)^\alpha \right\} \\ & + (\beta - 1) \sum_{i=1}^n \log \left[ 1 - \exp \left\{ - \left[ 1 - e^{-(x_i/\tau)^\alpha} \right] (x_i/\tau)^\alpha \right\} \right] \\ & - \lambda \sum_{i=1}^n \left\{ e^{\left[ 1 - e^{-(x_i/\tau)^\alpha} \right] (x_i/\tau)^\alpha} - 1 \right\}^\beta. \end{aligned} \quad (13)$$

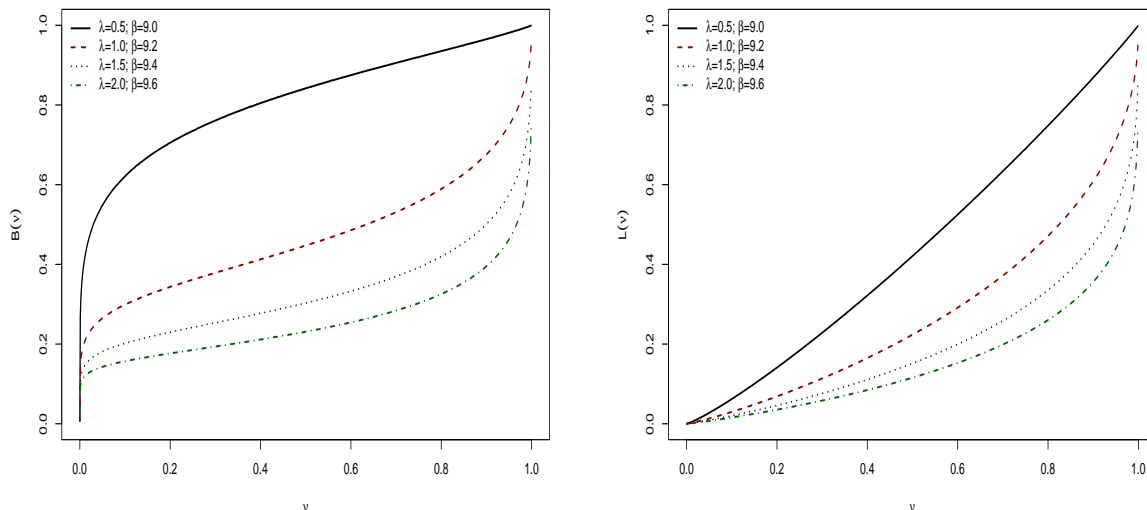


Figure 5: Bonferroni and Lorenz curves of MKFW( $\lambda, \beta, \alpha, \tau$ )

Maximizing numerically (13) gives the MLE of  $\theta$ .

#### 4.1. Regression model

The *log-modified Kies flexible Weibull* (LMKFW) distribution is obtained by the transformation  $Y = \log(X)$ , where  $X$  has pdf (3). Its density, reparameterized in terms of  $\alpha = 1/\sigma$  and  $\tau = e^\mu$ , has the form

$$\begin{aligned}
 f(y) &= \lambda \beta \sigma^{-1} e^{\left(\frac{y-\mu}{\sigma}\right) - e^{\left(\frac{y-\mu}{\sigma}\right)}} \exp \left\{ \beta \left[ 1 - e^{-e^{\left(\frac{y-\mu}{\sigma}\right)}} \right] e^{\left(\frac{y-\mu}{\sigma}\right)} \right\} \\
 &\quad \times \left[ 1 - \exp \left\{ - \left[ 1 - e^{-e^{\left(\frac{y-\mu}{\sigma}\right)}} \right] e^{\left(\frac{y-\mu}{\sigma}\right)} \right\} \right]^{\beta-1} \left\{ \left[ e^{e^{\left(\frac{y-\mu}{\sigma}\right)}} - 1 \right] + e^{\left(\frac{y-\mu}{\sigma}\right)} \right\} \\
 &\quad \times \exp \left\{ -\lambda \left[ e^{\left(1 - e^{-e^{\left[\frac{y-\mu}{\sigma}\right]}}\right) e^{\left(\frac{y-\mu}{\sigma}\right)}} - 1 \right]^\beta \right\}, \quad y \in \mathbb{R}, \tag{14}
 \end{aligned}$$

where  $\lambda, \beta, \sigma > 0$  and  $\mu \in \mathbb{R}$ . The density of  $Z = (Y - \mu)/\sigma$  can be written as

$$\begin{aligned}
 f(z) &= \lambda \beta e^{z - e^z} \exp \left[ \beta \left( 1 - e^{-e^z} \right) e^z \right] \left\{ 1 - \exp \left[ - \left( 1 - e^{-e^z} \right) e^z \right] \right\}^{\beta-1} \left[ \left( e^{e^z} - 1 \right) + e^z \right] \\
 &\quad \times \exp \left\{ -\lambda \left[ e^{\left(1 - e^{-e^z}\right) e^z} - 1 \right]^\beta \right\}, \quad z \in \mathbb{R}. \tag{15}
 \end{aligned}$$

Equation (15) represents the standard LMKFW density. A regression model can be constructed based on (14) to link the response variable  $y_i$  to the explanatory variable vector  $\mathbf{v}_i^\top = (v_{i1}, \dots, v_{ip})^\top$  as

$$y_i = \mathbf{v}_i^\top \boldsymbol{\eta} + \sigma z_i, \quad i = 1, \dots, n, \tag{16}$$

where  $\mu_i = \mathbf{v}_i^\top \boldsymbol{\eta}$ ,  $\boldsymbol{\eta} = (\eta_1, \dots, \eta_p)^\top$  is the vector of parameters of the regression model, and  $z_i$  denotes the random error with density (15).

The log-likelihood function for  $\boldsymbol{\zeta} = (\lambda, \beta, \sigma, \boldsymbol{\eta}^\top)^\top$  from Equations (15) and (16), can be derived by considering  $y_i = \min(Y_i, C_i)$ , where  $Y_i$  and  $C_i$  are independent random variables

representing the lifetime and non-informative censoring time, respectively. For right-censored data, it takes the form

$$\begin{aligned} \ell(\zeta) = & d [\log(\lambda) + \log(\beta) - \log(\sigma)] + \sum_{i \in F} z_i - \sum_{i \in F} e^{z_i} + \beta \sum_{i \in F} (1 - e^{-e^{z_i}}) e^{z_i} \\ & + (\beta - 1) \sum_{i \in F} \log \left\{ 1 - \exp \left[ - (1 - e^{-e^{z_i}}) e^{z_i} \right] \right\} + \sum_{i \in F} \log \left[ (e^{e^{z_i}} - 1) + e^{z_i} \right] \\ & - \lambda \sum_{i \in F} \left[ e^{(1 - e^{-e^{z_i}}) e^{z_i}} - 1 \right]^\beta - \lambda \sum_{i \in C} \left[ e^{(1 - e^{-e^{z_i}}) e^{z_i}} - 1 \right]^\beta, \end{aligned} \quad (17)$$

where  $d$  is the number of failures,  $z_i = (y_i - \mu_i)/\sigma$ , and  $F$  and  $C$  denote the sets of lifetimes and censoring times, respectively. The MLE of  $\zeta$  is found by numerically maximizing (17).

## 5. Simulations

To evaluate the accuracy of the MLEs derived from the MKFW distribution, random samples of sizes  $n = 50, 100, 200$ , and  $500$  are generated under three distinct scenarios using the Newton-Raphson algorithm. One thousand Monte Carlo replicates are conducted, and the average estimates (AEs), biases, and mean squared errors (MSEs) are computed. To optimize Equation (13), the Broyden-Fletcher-Goldfarb-Shannon (BFGS) numerical method is used. This method is implemented using the `Optim` function of the R statistical software, with the true values of the parameters as initial inputs.

To generate MKFW variates, the Newton-Raphson algorithm involves the steps:

1. Set  $\lambda, \beta, \alpha, \tau$ , and  $x^0$ .
2. Generate  $u \sim \text{Uniform}(0, 1)$ .
3. Update  $x^0$  by using Newton's formula

$$x^* = x^0 - \frac{F(x^0) - u}{f(x^0)},$$

where  $F(\cdot)$  is the MKFW cdf obtained from (1), and  $f(\cdot)$  is the pdf (3).

4. While  $|x^0 - x^*| > \epsilon$ , where  $\epsilon$  is a small tolerance limit, set  $x^0 = x^*$  and return to step 3. Otherwise, set  $x^0 = x^*$  as a variable from the MKFW distribution.
5. The steps 2-4 are repeated  $n$  times to generate variates from the MKFW distribution.

The numbers in Table 1 reveal that the estimators of the MKFW parameters are consistent since the AEs approach their true values and the biases and MSEs approach zero with increasing sample size. Further, the last two quantities vary across scenarios, thus indicating that the accuracy of the estimators may be affected by the selected parameters, especially for smaller sample sizes.

The accuracy of the MLEs in the regression model is evaluated using 1,000 Monte Carlo replicates for  $n = 50, 100, 200$ , and  $500$  under the acceptance-rejection method, and  $\lambda = 0.5, \beta = 0.4, \sigma = 4.0, \eta_0 = 1.5, \eta_1 = 2.5$ . The censoring times  $c_1, \dots, c_n$  are generated using a uniform distribution  $(0, b)$ , where  $b$  determines the censoring percentage (0%, 10%, 30%). Equation (17) is optimized using the Nelder-Mead numerical method run with the `Optim` function in R, with the true values of the parameters serving as initial inputs.

The simulation process is described as (for  $i = 1, \dots, n$ ):

1. Generate  $v_{i1} \sim \text{Uniform}(0, 1)$  and set  $\mu_i = \eta_0 + \eta_1 v_{i1}$ .
2. Generate  $t_i$  from  $w(t_i) = (1/\sigma) \exp \{ (t_i - \mu_i)/\sigma - \exp [(t_i - \mu_i)/\sigma] \}$ .



Table 1: Simulations from the MKFW distribution

$n$	$\theta$	(1.2, 0.5, 0.8, 0.3)			(0.2, 0.7, 1.2, 0.1)			(0.5, 0.6, 0.9, 0.2)		
		AE	Bias	MSE	AE	Bias	MSE	AE	Bias	MSE
50	$\lambda$	1.4569	0.2569	1.0763	0.6197	0.4197	0.6025	0.9047	0.4047	0.7605
	$\beta$	0.4047	-0.0952	0.1864	0.5979	-0.1020	0.4436	0.4790	-0.1209	0.1940
	$\alpha$	1.6468	0.8468	1.6589	2.5546	1.3546	5.9504	1.9010	1.0010	2.7889
	$\tau$	0.3882	0.0882	0.0823	0.1492	0.0492	0.0075	0.2985	0.0985	0.0456
100	$\lambda$	1.4018	0.2018	0.8253	0.4916	0.2916	0.3056	0.7944	0.2944	0.4787
	$\beta$	0.4625	-0.0374	0.1401	0.6047	-0.0952	0.1560	0.5216	-0.0783	0.1167
	$\alpha$	1.3343	0.5343	0.9112	2.0227	0.8227	2.6646	1.4982	0.5982	1.3301
	$\tau$	0.3693	0.0693	0.0650	0.1372	0.0372	0.0053	0.2714	0.0714	0.0319
200	$\lambda$	1.3247	0.1247	0.4777	0.3845	0.1845	0.1550	0.6856	0.1856	0.2835
	$\beta$	0.4874	-0.0125	0.1055	0.6361	-0.0638	0.1252	0.5508	-0.0491	0.0661
	$\alpha$	1.1109	0.3109	0.4389	1.6274	0.4274	0.8270	1.2230	0.3230	0.5455
	$\tau$	0.3450	0.0450	0.0387	0.1267	0.0267	0.0030	0.2462	0.0462	0.0204
500	$\lambda$	1.2551	0.0551	0.2281	0.2894	0.0894	0.0383	0.5806	0.0806	0.0884
	$\beta$	0.4982	-0.0017	0.0560	0.6573	-0.0426	0.0210	0.5770	-0.0229	0.0293
	$\alpha$	0.9606	0.1606	0.1971	1.3915	0.1915	0.1878	1.0314	0.1314	0.1545
	$\tau$	0.3210	0.0210	0.0193	0.1155	0.0155	0.0012	0.2206	0.0206	0.0085

3. Generate  $u \sim \text{Uniform}(0, 1)$ .
4. If  $u \leq f(t_i)/Mw(t_i)$ , then  $y_i = t_i$ , where  $f(\cdot)$  comes from (15) and (16), and  $M = \max [f(t_i)/w(t_i)]$ . Otherwise, return to step 2.
5. Generate  $c_i \sim \text{Uniform}(0, b)$ .
6. The observed times are  $y_i^* = \min(y_i, c_i)$ , where the censoring indicator  $\delta_i = 1$  if  $y_i \leq c_i$  and  $\delta_i = 0$ , otherwise.

The results in Table 2 demonstrate the consistency of the estimators in the regression model, where the AEs converge to the true parameters, and the biases and MSEs approach zero when  $n$  increases. However, the last two quantities also increase if the censoring percentage grows, thus highlighting the impact of censoring on reducing the accuracy of the estimators. All simulations are implemented in R.

## 6. Applications

### 6.1. COVID-19 data in Pernambuco (Brazil)

The emergence of the novel coronavirus, Severe Acute Respiratory Syndrome Coronavirus 2 (SARS-CoV-2), in late 2019 led to the rapid spread of COVID-19, a highly contagious respiratory disease, in early 2020. This unforeseen pandemic has resulted in a significant loss of life and has prompted governments around the world to implement unprecedented measures to protect their citizens.

In the state of Pernambuco (located in the northeastern region of Brazil), the COVID-19 situation has presented significant challenges. A substantial number of infections and deaths have been confirmed in the state, which is the seventh most populous in Brazil and has the tenth highest gross domestic product (GDP) in the country. In addition, Pernambuco has the highest GDP per capita among the states of the Northeast region. Recently, the state

Table 2: Simulations from the LMKFW regression model

$n$	$\zeta$	0%			10%			30%		
		AE	Bias	MSE	AE	Bias	MSE	AE	Bias	MSE
50	$\lambda$	0.6686	0.1686	0.1651	0.6565	0.1565	0.2669	0.7146	0.2146	0.7711
	$\beta$	0.3615	-0.0384	0.0665	0.3646	-0.0353	0.0692	0.4070	0.0070	0.4421
	$\sigma$	3.4504	-0.5495	3.5255	3.4843	-0.5156	4.3816	3.8639	-0.1360	29.0084
	$\eta_0$	2.0666	0.5666	3.5561	2.0950	0.5950	3.2851	1.9851	0.4851	3.5426
	$\eta_1$	2.7161	0.2161	3.0472	2.7842	0.2842	4.7793	3.0638	0.5638	7.7924
100	$\lambda$	0.6098	0.1098	0.0882	0.6069	0.1069	0.0782	0.6053	0.1053	0.1373
	$\beta$	0.3739	-0.0260	0.0194	0.3628	-0.0371	0.0201	0.3703	-0.0296	0.0721
	$\sigma$	3.6758	-0.3241	1.7010	3.5610	-0.4389	1.7200	3.6258	-0.3741	5.8014
	$\eta_0$	1.8203	0.3203	2.3751	1.9147	0.4147	2.5261	1.9031	0.4031	2.7891
	$\eta_1$	2.6385	0.1385	2.4440	2.7517	0.2517	4.2041	2.7369	0.2369	4.3922
200	$\lambda$	0.5751	0.0751	0.0561	0.5804	0.0804	0.0564	0.5749	0.0749	0.0535
	$\beta$	0.3783	-0.0216	0.0106	0.3759	-0.0240	0.0120	0.3743	-0.0256	0.0236
	$\sigma$	3.7630	-0.2369	1.1339	3.7240	-0.2759	1.1799	3.7139	-0.2860	2.1106
	$\eta_0$	1.7642	0.2642	1.9917	1.7141	0.2141	1.8125	1.7155	0.2155	1.9066
	$\eta_1$	2.5264	0.0264	2.0362	2.7578	0.2578	4.3331	2.7520	0.2520	3.9626
500	$\lambda$	0.5327	0.0327	0.0234	0.5344	0.0344	0.0239	0.5385	0.0385	0.0267
	$\beta$	0.3921	-0.0078	0.0050	0.3909	-0.0090	0.0057	0.3867	-0.0132	0.0096
	$\sigma$	3.9220	-0.0779	0.6030	3.9051	-0.0948	0.6263	3.8642	-0.1357	0.9965
	$\eta_0$	1.5848	0.0848	1.0907	1.5424	0.0424	0.9666	1.5597	0.0597	1.1011
	$\eta_1$	2.5043	0.0043	1.1630	2.6405	0.1405	2.9303	2.6786	0.1786	3.1722

has seen an increase in the number of cases, along with an increase in the test positivity rate. Despite this increase in numbers, most cases are classified as mild.

In this context, the data set under consideration comprises the recovery times (in days) of 248 individuals diagnosed with COVID-19 in the year 2022 within the state, which can be accessed at <https://github.com/alexaaf31/The-Modified-kies-Flexible-Generalized-Family>. The data set reveals an average recovery time of 28.915 days and a standard deviation of 20.419. The skewness and kurtosis are 0.606 and 2.376, which suggest that the data are right-skewed and platykurtic.

The MKFW distribution is fitted with other well-established distributions, such as the *Kw Weibull* (KwW) (Cordeiro, Ortega, and Nadarajah 2010), *beta Weibull* (BW) (Lee, Famoye, and Olumolade 2007), *Weibull Weibull* (WW) (Bourguignon *et al.* 2014), *Lomax Weibull* (LW) (Cordeiro, Afify, Ortega, Suzuki, and Mead 2019), *gamma Weibull* (GW) (Nadarajah, Cordeiro, and Ortega 2015), and *Weibull* (W).

Table 3 reports the MLEs and standard errors (SEs) (in parentheses) of the distributions fitted to these data, where all of them (except BW) have accurate estimates. The results in Table 4 demonstrate that the MKFW distribution outperforms the other distributions, as evidenced by the lower values of Cramér-von Mises ( $W^*$ ), Anderson-Darling ( $A^*$ ), Akaike information criterion (AIC), consistent AIC (CAIC), Bayesian information criterion (BIC), Hannan-Quinn IC (HQIC), and Kolmogorov-Smirnov (KS) along its corresponding  $p$ -value. The statistics  $W^*$  and  $A^*$  are defined by Chen and Balakrishnan (1995).

Considering only the distributions with accurate estimates, the generalized likelihood ratio (GLR) test (Vuong 1989) compares the MKFW model with the KwW (GLR = 11.842), WW (GLR = 22.452), LW (GLR = 16.997), GW (GLR = 13.618), and WE (GLR = 16.475) models at a significance level of 5%. The results of the GLR tests indicate that the MKFW model provides a superior fit to the current data compared to the alternatives. Figure 6 confirms

Table 3: Results for COVID-19 data in Pernambuco

Model	MLEs (SEs)			
MKFW( $\lambda, \beta, \alpha, \phi$ )	1.554 (0.099)	0.164 (0.009)	3.835 (0.059)	46.605 (0.048)
KwW( $a, b, \alpha, \phi$ )	0.149 (0.010)	1.961 (0.183)	7.208 (0.015)	81.476 (0.015)
BW( $a, b, \alpha, \phi$ )	0.385 (0.165)	0.718 (0.539)	2.633 (0.899)	43.132 (20.364)
WW( $\lambda, \beta, \alpha, \phi$ )	0.007 (0.002)	0.510 (0.112)	0.302 (0.022)	0.019 (0.006)
LW( $\lambda, \beta, \alpha, \phi$ )	0.088 (0.007)	6.528 (2.592)	1.013 (0.010)	2.322 (0.005)
GW( $a, \alpha, \beta$ )	0.332 (0.145)	3.022 (1.024)	58.171 (7.820)	
WE( $\alpha, \phi$ )	0.032 (0.002)	1.383 (0.071)		

this fact visually through the close correspondence between the pdf and cdf estimated by the model and the histogram and empirical cdf of the data.

All previous results are done with the `AdequacyModel` (Marinho, Silva, Bourguignon, Cordeiro, and Nadarajah 2019) script in R package with the BFGS algorithm.

Table 4: Adequacy measures for COVID-19 data in Pernambuco

Model	$W^*$	$A^*$	AIC	CAIC	BIC	HQIC	KS	$p$ -value
MKFW	0.071	0.520	2119.820	2119.985	2133.874	2125.478	0.045	0.693
KwW	0.114	0.848	2126.131	2126.295	2140.184	2131.788	0.059	0.352
WW	0.247	1.723	2146.838	2147.002	2160.891	2152.495	0.063	0.269
LW	0.373	2.307	2153.241	2153.406	2167.295	2158.899	0.083	0.060
GW	0.154	1.079	2130.354	2130.453	2140.895	2134.597	0.067	0.206
WE	0.190	1.217	2134.018	2134.067	2141.045	2136.847	0.057	0.376

## 6.2. Stress data

The bimodal capability of the MKFW distribution is explored by comparing it with other flexible models capable of exhibiting this shape. These models include the *Kw flexible Weibull* (KwFW) (M.A.El-Damcese, Mustafa, B.S.El-Desouky, and M.E.Mustafa 2016), *generalized odd log-logistic Weibull* (GOLLW) (Cordeiro, Alizadeh, Ozel, Hosseini, Ortega, and Altun 2017), *Weibull Marshall-Olkin Weibull* (WMOW) (Korkmaz, Cordeiro, Yousof, Pescim, Afify, and Nadarajah 2019), and *extended Weibull log-logistic* (EWLL) (Abouelmagd, Hamed, Al-mamy, Ali, Yousof, Korkmaz *et al.* 2019) models.

Accelerated life testing is a technique used to estimate the useful life of a product by subjecting it to more severe levels of stress than it would suffer in normal use. This speeds up the failure process, allowing researchers to collect failure data in a shorter period of time compared to its use under normal conditions. Thus, this analysis shows the flexibility of the MKFW distribution to fit the data set 12.2 from Murthy, Xie, and Jiang (2004), which refers to the accelerated life testing of 40 items (with a change in stress from 100 to 150 at  $t = 15$ ). The data are: 0.13, 0.62, 0.75, 0.87, 1.56, 2.28, 3.15, 3.25, 3.55, 4.49, 4.50, 4.61, 4.79, 7.17, 7.31, 7.43, 7.84, 8.49, 8.94, 9.40, 9.61, 9.84, 10.58, 11.18, 11.84, 13.28, 14.47, 14.79, 15.54, 16.90,

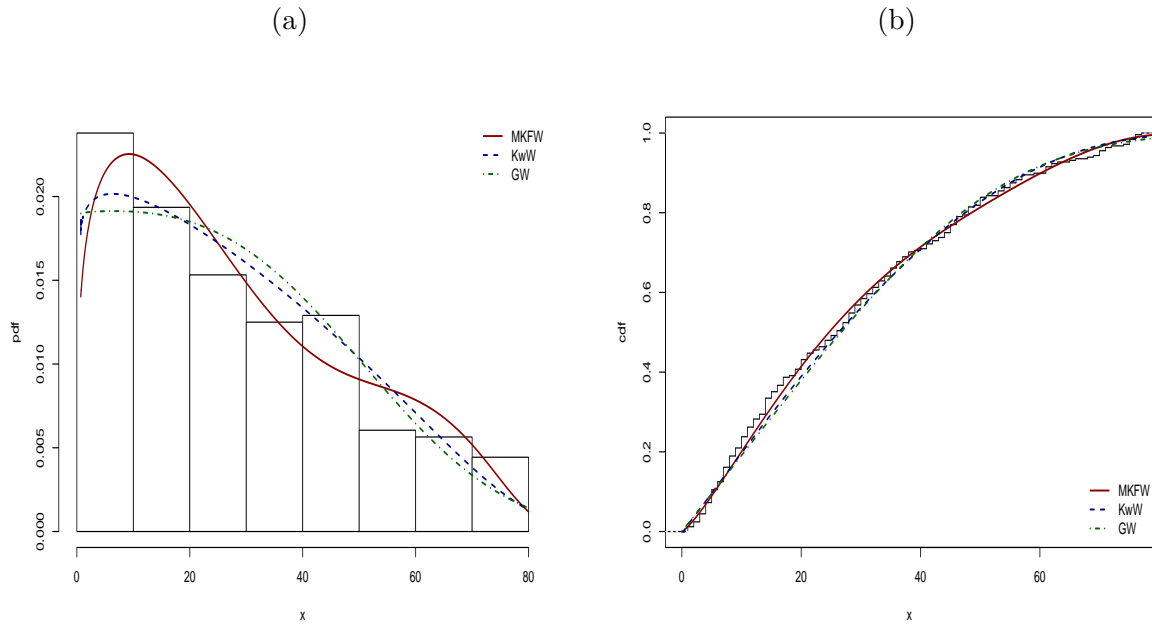


Figure 6: Estimated pdfs (a) and cdfs (b) for COVID-19 data in Pernambuco

17.25, 17.37, 18.69, 18.78, 19.88, 20.06, 20.10, 20.95, 21.72, 23.87.

Table 5: Results for stress data

Model	MLEs (SEs)			
MKFW( $\lambda, \beta, \alpha, \phi$ )	0.908 (0.155)	0.142 (0.018)	3.687 (0.011)	12.154 (0.011)
KwFW( $a, b, \alpha, \beta$ )	0.244 (0.101)	0.119 (0.020)	0.151 (0.002)	1.822 (0.003)
GOLLW( $\alpha, \theta, a, b$ )	0.640 (0.105)	0.236 (0.055)	5.845 (0.140)	17.721 (0.119)
WMOW( $\alpha, \beta, \gamma, \theta$ )	4.348 (4.915)	0.883 (0.638)	1.141 (0.968)	6.207 (5.108)
EWLL( $\lambda, \alpha, \beta$ )	0.232 (0.088)	0.681 (0.094)	6.477 (2.237)	

The skewness (0.220) and kurtosis (1.810) support that the data are right-skewed and platykurtic. Table 5 reports the MLEs and SEs for the fitted models, which are also obtained using the `AdequacyModel` package in R with the BFGS algorithm. The estimates for the MKFW, KwFW, GOLLW, and EWLL distributions are accurate. The MKFW distribution has the lowest values of the adequacy measures given in Table 6. The GLR tests comparing the MKFW model against the KwFW (GLR = 2.561), GOLLW (GLR = 2.767), WMOW (GLR = 4.311), and EWLL (GLR = 5.107) models for a significance level of 5% validate the best fit of the MKFW model to the data. Figure 7 illustrates that the estimated pdf and cdf of the MKFW distribution are closest to the histogram and the empirical cumulative distribution.

### 6.3. COVID-19 data in Rondonópolis, Brazil

Like Pernambuco, the city of Rondonópolis in the state of Mato Grosso (center-west region of Brazil) has endured significant challenges during the COVID-19 pandemic, with a considerable number of infections and deaths attributed to the virus. Located about 210 km from the cap-

Table 6: Adequacy measures for stress data

Model	$W^*$	$A^*$	AIC	CAIC	BIC	HQIC	KS	$p$ -value
MKFW	0.023	0.151	260.654	261.797	267.409	263.096	0.079	0.945
KwFW	0.070	0.409	264.360	265.503	271.115	266.802	0.096	0.811
GOLLW	0.032	0.184	261.400	262.543	268.155	263.842	0.086	0.899
WMOW	0.060	0.458	269.131	270.274	275.886	271.573	0.088	0.882
EWLL	0.096	0.683	269.831	270.497	274.897	271.663	0.087	0.893

(a)

(b)

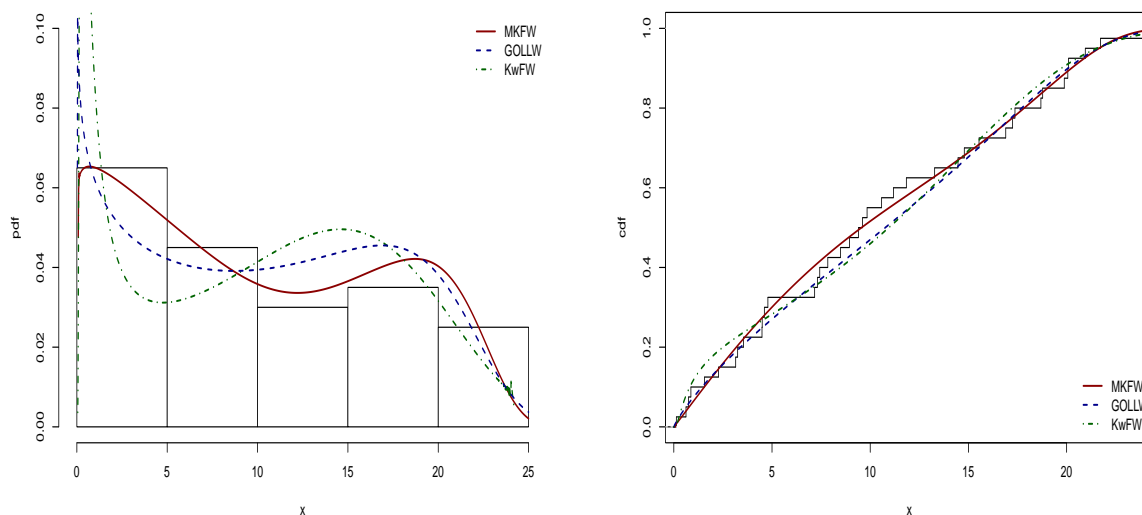


Figure 7: Estimated pdfs (a) and cdfs (b) for stress data

ital of Cuiabá, Rondonópolis is a significant economic hub, holding the second-highest GDP in Mato Grosso. Its strategic position at the intersection of the BR-163 and BR-364 highways designates it a crucial link between Brazil's northern and southern regions, facilitating the transportation of both agricultural and industrial goods to major cities and ports nationwide. This data set contains the lifetime (in days) of 370 individuals diagnosed with COVID-19 in Rondonópolis during 2020, which can be accessed at <https://github.com/alexaaf31/The-Modified-kies-Flexible-Generalized-Family/blob/main/RONCOVID.csv>.

The response variable  $y_i$  denotes the time between the onset of symptoms and the death of the patient due to COVID-19. Approximately 60.27% of the observations are censored, corresponding to patients who died from other causes or survived past the study period. The variables (for  $i = 1, \dots, 370$ ) are:  $\delta_i$ : censoring indicator (0 = censored, 1 = observed lifetime),  $v_{i1}$ : age (in years), and  $v_{i2}$ : cardiovascular diseases (1 = yes, 0 = no or not informed). Figure 8(a) shows that individuals between the ages of 40 and 80 have the highest frequency of hospitalizations. Figure 8(b) indicates that cardiovascular disease is associated with a higher risk of death from COVID-19.

The regression model proposed for these data is

$$y_i = \eta_0 + \eta_1 v_{i1} + \eta_2 v_{i2} + \sigma z_i, \quad i = 1, \dots, 370,$$

where  $z_i$  has pdf (15). The findings are compared with those of the *log-Kw Weibull* (LKwW), *log-beta Weibull* (LBW) (Ortega, Cordeiro, and Kattan 2013), and *log-Weibull Weibull* (LWW) regressions. The MLEs, the corresponding SEs in parentheses, and the  $p$ -values in brackets of the selected regression models are obtained using a script in R via the `Optim` function with

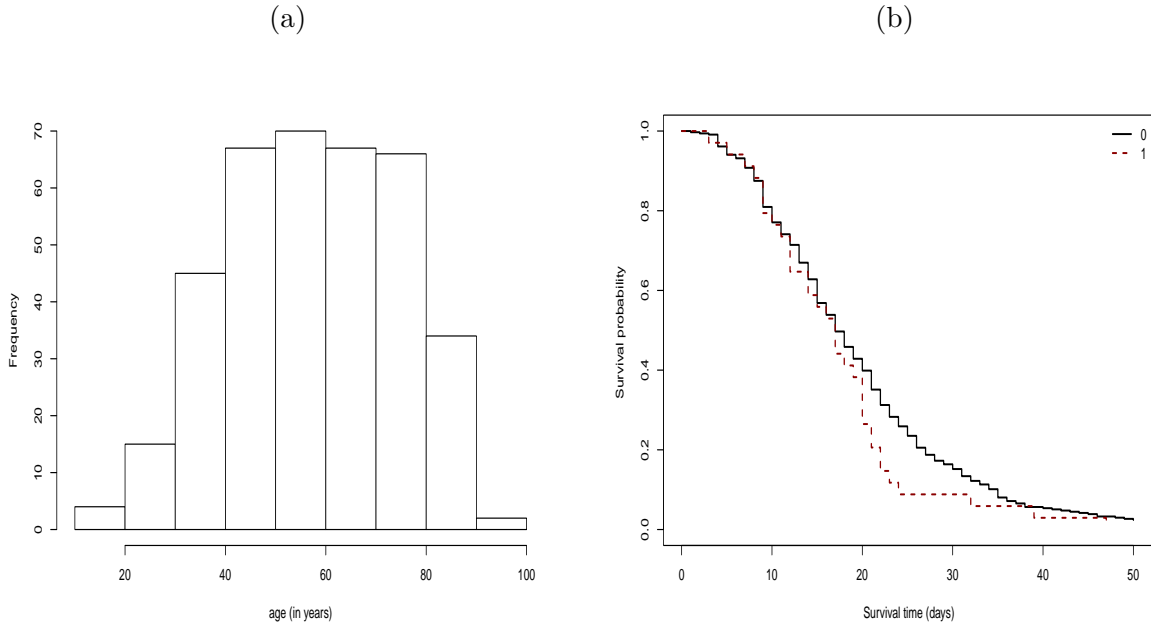


Figure 8: Histogram for age (a) and Kaplan-Meier curves for cardiovascular disease (b) for COVID-19 data in Rondonópolis

the BFGS algorithm. Then, the numbers in Table 7 show that age and cardiovascular disease significantly decrease the time to death at the 5% level because of the negative signs of  $\eta_1$  and  $\eta_2$ .

The results of the GLR tests comparing the LMKFW regression with the LKwW (GLR = 55.130), LBW (GLR = 75.524), and LWW (GLR = 67.576) regressions, and the figures in Table 8, show that the LMKFW regression exhibits a superior fit to the current data. The quantile residuals (qrs) (Dunn and Smyth 1996) to analyze the fit of this regression are given by

$$qr_i = \Phi^{-1} \left( 1 - \exp \left\{ -\hat{\lambda} \left[ e^{\left(1 - e^{-\hat{z}_i}\right) e^{\hat{z}_i}} - 1 \right]^{\hat{\beta}} \right\} \right),$$

where  $\Phi^{-1}(\cdot)$  is the standard normal quantile function,  $\hat{z}_i = (y_i - \hat{\mu}_i)/\hat{\sigma}$ , and  $\hat{\mu} = \mathbf{v}_i^\top \hat{\boldsymbol{\eta}}$ . According to Figure 9, the qrs are randomly distributed and follow approximately a standard normal distribution. Hence, the LMKFW regression model explains the COVID-19 data in Rondonópolis.

The computational routine implemented in R is available online at <https://github.com/alexaaf31/The-Modified-kies-Flexible-Generalized-Family>.

## 7. Conclusions

This paper introduced the modified Kies flexible generalized (MKF-G) family, which expands the modeling capabilities of its baseline distributions by incorporating bimodal and bathtub shapes. A special case of this family, the modified Kies flexible Weibull distribution, is examined in detail. We explored its properties and developed a regression model for censored data. The simulations proved the consistency of the maximum likelihood estimators. The models in the new family outperformed those from the well-known Kumaraswamy-G, beta-G, and Weibull-G classes for three real data sets, thus providing a new tool for modeling bimodal and bathtub shape data.

Table 7: Results for COVID-19 data in Rondonópolis

Model	$\lambda$	$\beta$	$\sigma$	$\eta_0$	$\eta_1$	$\eta_2$
LMKFW	2.403 (0.587)	0.219 (0.015)	0.231 (0.006)	5.083 (0.004) [< 0.001]	-0.016 (0.001) [< 0.001]	-0.310 (0.105) [0.003]
LKwW	1.331 (0.561)	0.551 (1.648)	0.630 (0.202)	4.182 (1.568) [0.007]	-0.016 (0.003) [< 0.001]	-0.302 (0.128) [0.019]
LBW	1.401 (0.729)	1.152 (2.725)	0.671 (0.237)	4.574 (1.391) [0.001]	-0.017 (0.003) [< 0.001]	-0.296 (0.129) [0.022]
LWW	0.030 (0.062)	4.022 (1.674)	3.443 (1.343)	3.934 (1.125) [< 0.001]	-0.016 (0.003) [< 0.001]	-0.267 (0.113) [0.018]

Table 8: Adequacy measures for COVID-19 data in Rondonópolis

Model	AIC	CAIC	BIC	HQIC
LMKFW	524.285	524.684	547.766	533.612
LKwW	524.843	525.241	548.324	534.170
LBW	524.892	525.291	548.373	534.219
LWW	528.605	529.004	552.086	537.932

(a)

(b)

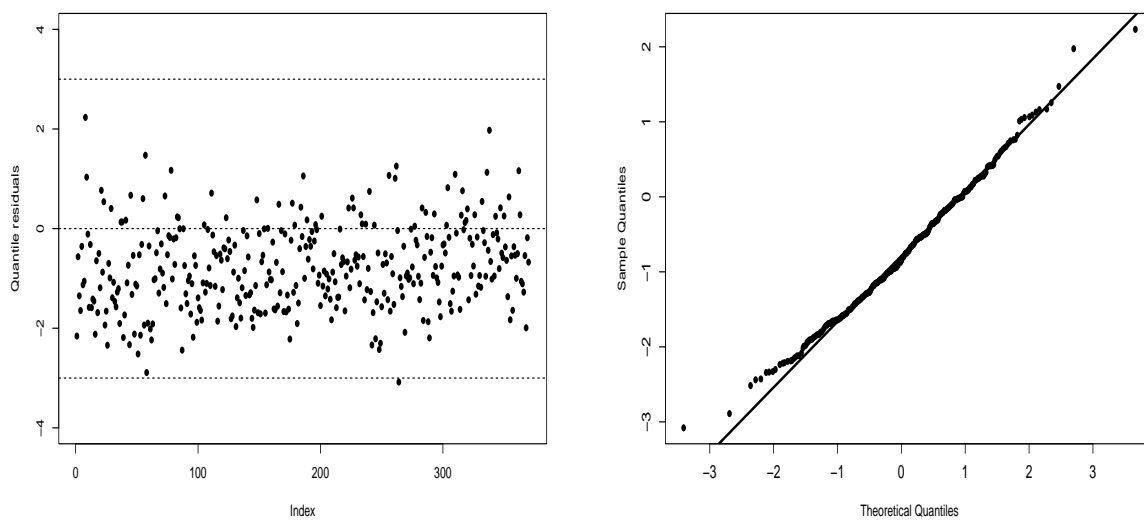


Figure 9: Index plot (a) and normal probability plot (b) for COVID-19 data in Rondonópolis

### Acknowledgments

We thank the reviewers for their helpful comments. This work is supported by Fundação de Amparo à Ciência e Tecnologia do Estado de Pernambuco (FACEPE) [IBPG-1448-1.02/20].

## References

- Abouelmagd THM, Hamed MS, Almamy JA, Ali MM, Yousof HM, Korkmaz MC, *et al.* (2019). “Extended Weibull Log-Logistic Distribution.” *Journal of Nonlinear Sciences and Applications*, **12**, 523–534. doi:10.22436/jnsa.012.08.03.
- Alexander C, Cordeiro GM, Ortega EMM, Sarabia J (2012). “Generalized Beta-Generated Distributions.” *Computational Statistics & Data Analysis*, **56**, 1880–1897. doi:10.2139/ssrn.1650630.
- Alizadeh M, Emadi M, Doostparast M, Cordeiro GM, Ortega EMM, Pescim RR (2015). “A New Family of Distributions: The Kumaraswamy Odd Log-Logistic, Properties and Applications.” *Hacetatepe Journal of Mathematics and Statistics*, **44**, 1491–1512. doi:10.15672/HJMS.2014418153.
- Alzaatreh A, Lee C, Famoye F (2013). “A New Method For Generating Families of Continuous Distributions.” *METRON*, **71**, 63–79. doi:10.1007/s40300-013-0007-y.
- Baharith LA, Alamoudi HH (2021). “The Exponentiated Fréchet Generator of Distributions with Applications.” *Symmetry*, **13**, 572. doi:10.3390/sym13040572.
- Bourguignon M, Silva R, Cordeiro GM (2014). “The Weibull-G Family of Probability Distributions.” *Journal of Data Science*, **12**, 53–68. doi:10.6339/JDS.201401\_12(1).0004.
- Chen G, Balakrishnan N (1995). “A General Purpose Approximate Goodness-of-Fit Test.” *Journal of Quality Technology*, **27**, 154–161. doi:10.1080/00224065.1995.11979578.
- Chipepa F, Oluyede BO, Makubate B (2019). “A New Generalized Family of Odd Lindley-G Distributions with Application.” *International Journal of Statistics and Probability*, **8**, 1–22. doi:10.5539/ijsp.v8n6p1.
- Cordeiro GM, Afify AZ, Ortega EMM, Suzuki AK, Mead ME (2019). “The Odd Lomax Generator of Distributions: Properties, Estimation and Applications.” *Journal of Computational and Applied Mathematics*, **347**, 222–237. doi:10.1016/j.cam.2018.08.008.
- Cordeiro GM, Alizadeh M, Ozel G, Hosseini B, Ortega EMM, Altun E (2017). “The Generalized Odd Log-Logistic Family of Distributions: Properties, Regression Models and Applications.” *Journal of Statistical Computation and Simulation*, **87**, 908–932. doi:10.1080/00949655.2016.1238088.
- Cordeiro GM, de Castro M (2011). “A New Family of Generalized Distributions.” *Journal of Statistical Computation and Simulation*, **81**, 883–898. doi:10.1080/00949650903530745.
- Cordeiro GM, Ortega EMM, Cunha DCC (2013). “The Exponentiated Generalized Class of Distributions.” *Journal of Data Science*, **11**, 1–27. doi:10.6339/JDS.2013.11(1).1086.
- Cordeiro GM, Ortega EMM, Nadarajah S (2010). “The Kumaraswamy Weibull Distribution with Application to Failure Data.” *Journal of the Franklin Institute*, **347**, 1399–1429. doi:10.1016/j.jfranklin.2010.06.010.
- Dunn PK, Smyth GK (1996). “Randomized Quantile Residuals.” *Journal of Computational and Graphical Statistics*, **5**, 236–244. doi:10.2307/1390802.
- Eugene N, Lee C, Famoye F (2002). “Beta-Normal Distribution and Its Applications.” *Communications in Statistics - Theory and Methods*, **31**, 497–512. doi:10.1081/STA-120003130.



- Gupta RC, Gupta PL, Gupta RD (1998). "Modeling Failure Time Data by Lehman Alternatives." *Communications in Statistics - Theory and Methods*, **27**, 887–904. doi: [10.1080/03610929808832134](https://doi.org/10.1080/03610929808832134).
- Gupta RD, Kundu D (2001). "Exponentiated Exponential Family: An Alternative to Gamma and Weibull Distributions." *Biometrical Journal: Journal of Mathematical Methods in Biosciences*, **43**, 117–130. doi:[10.1002/1521-4036\(200102\)43:1<117::AID-BIMJ117>3.0.CO;2-R](https://doi.org/10.1002/1521-4036(200102)43:1<117::AID-BIMJ117>3.0.CO;2-R).
- Korkmaz MÇ, Cordeiro GM, Yousof HM, Pescim RR, Afify AZ, Nadarajah S (2019). "The Weibull Marshall-Olkin Family: Regression Model and Application to Censored Data." *Communications in Statistics-Theory and Methods*, **48**, 4171–4194. doi:[10.1080/03610926.2018.1490430](https://doi.org/10.1080/03610926.2018.1490430).
- Kumar CS, Dharmaja SHS (2017). "On Modified Kies Distribution and Its Applications." *Journal of Statistical Research*, **51**, 41–60. doi:[10.47302/jsr.2017510103](https://doi.org/10.47302/jsr.2017510103).
- Lee C, Famoye F, Olumolade O (2007). "Beta-Weibull Distribution: Some Properties and Applications to Censored Data." *Journal of Modern Applied Statistical Methods*, **6**, 17. doi:[10.22237/jmasm/1177992960](https://doi.org/10.22237/jmasm/1177992960).
- MAEl-Damcese, Mustafa A, BSEI-Desouky, MEMustafa (2016). "The Kumaraswamy Flexible Weibull Extension." *International Journal of Mathematics And its Applications*, **4**, 1–14.
- Marinho PRD, Silva RB, Bourguignon M, Cordeiro GM, Nadarajah S (2019). "Adequacy-Model: An R package for Probability Distributions and General Purpose Optimization." *PLOS ONE*, **14**, 1–30. doi:[10.1371/journal.pone.0221487](https://doi.org/10.1371/journal.pone.0221487).
- Marshall AW, Olkin I (1997). "A New Method for Adding a Parameter to a Family of Distributions with Application to the Exponential and Weibull Families." *Biometrika*, **84**, 641–652. doi:[10.1093/biomet/84.3.641](https://doi.org/10.1093/biomet/84.3.641).
- Mudholkar GS, Srivastava DK (1993). "Exponentiated Weibull Family for Analyzing Bathtub Failure-Rate Data." *IEEE Transactions on Reliability*, **42**, 299–302. doi:[10.1109/24.229504](https://doi.org/10.1109/24.229504).
- Munir AUKM (2013). *Series Representations and Approximation of Some Quantile Functions Appearing in Finance*. Ph.D. thesis, Department of Mathematics, University College London.
- Murthy DP, Xie M, Jiang R (2004). *Weibull Models*. John Wiley and Sons.
- Nadarajah S, Cordeiro GM, Ortega EMM (2015). "The Zografos–Balakrishnan-G Family of Distributions: Mathematical Properties and Applications." *Communications in Statistics - Theory and Methods*, **44**, 186–215. doi:[10.1080/03610926.2012.740127](https://doi.org/10.1080/03610926.2012.740127).
- Nadarajah S, Gupta AK (2005). "On the Moments of the Exponentiated Weibull Distribution." *Communications in Statistics - Theory and Methods*, **34**, 253–256. doi: [10.1080/03610920509342418](https://doi.org/10.1080/03610920509342418).
- Nadarajah S, Gupta AK (2007). "The Exponentiated Gamma Distribution with Application to Drought Data." *Calcutta Statistical Association Bulletin*, **59**, 29–54. doi:[10.1177/0008068320070103](https://doi.org/10.1177/0008068320070103).
- Nadarajah S, Kotz S (2003). "The Exponentiated Fréchet Distribution." *Interstat Electronic Journal*, **14**, 01–07.
- Ortega EMM, Cordeiro GM, Kattan MW (2013). "The Log-Beta Weibull Regression Model with Application to Predict Recurrence of Prostate Cancer." *Statistical Papers*, **54**, 113–132. doi:[10.1007/s00362-011-0414-1](https://doi.org/10.1007/s00362-011-0414-1).

- R Core Team (2023). *R: A Language and Environment for Statistical Computing*. R Foundation for Statistical Computing, Vienna, Austria. URL <https://www.R-project.org/>.
- Tahir MH, Hussain MA, Cordeiro GM (2022). “A New Flexible Generalized Family for Constructing Many Families of Distributions.” *Journal of Applied Statistics*, **49**, 1615–1635. doi:10.1080/02664763.2021.1874891.
- Tahir MH, Nadarajah S (2015). “Parameter Induction in Continuous Univariate Distributions: Well-Established G Families.” *Anais da Academia Brasileira de Ciências*, **87**, 539–568. doi:10.1590/0001-3765201520140299.
- Tlhaloganyang BP, Sengweni W, Oluyede B (2022). “The Gamma Odd Burr X-G Family of Distributions with Applications.” *Pakistan Journal of Statistics and Operation Research*, **18**, 721–746. doi:10.18187/pjsor.v18i3.4045.
- Vuong QH (1989). “Likelihood Ratio Tests for Model Selection and Non-Nested Hypotheses.” *Econometrica*, **57**, 307–333. doi:10.2307/1912557.
- Zografos K, Balakrishnan N (2009). “On Families of Beta-and Generalized Gamma-Generated Distributions and Associated Inference.” *Statistical Methodology*, **6**, 344–362. ISSN 1572-3127. doi:10.1016/j.stamet.2008.12.003.

#### Affiliation:

Alexsandro A. Ferreira  
 Department of Statistics  
 Federal University of Pernambuco  
 Recife, Brazil, 50670-901  
 E-mail: [alexsandro.ferreira.aaf@gmail.com](mailto:alexsandro.ferreira.aaf@gmail.com)

Gauss M. Cordeiro  
 Department of Statistics  
 Federal University of Pernambuco  
 Recife, Brazil, 50670-901  
 E-mail: [gauss@de.ufpe.br](mailto:gauss@de.ufpe.br)  
 URL: [https://pt.wikipedia.org/wiki/Gauss\\_Moutinho\\_Cordeiro](https://pt.wikipedia.org/wiki/Gauss_Moutinho_Cordeiro)